

Core-shell Si/C nanocomposite as anode material for lithium ion batteries*

Tao Zhang, Lijun Fu, Jie Gao, Lichun Yang, Yuping Wu, and Hoqing Wu

Department of Chemistry & Shanghai Key Laboratory of Molecular Catalysis and Innovative Materials, Fudan University, Shanghai 200433, China

Abstract: We report an effective method for the synthesis of a core-shell Si/C nanocomposite, and its application as anode material for lithium ion (Li-ion) batteries. Polyacrylonitrile (PAN)-coated Si nanoparticles are formed by emulsion polymerization, and this precursor is heat-treated under argon to generate a Si/C core-shell nanocomposite. The conductive carbon shell envelops the silicon nanoparticles and suppresses aggregation of the nanoparticles during cycling. Meanwhile, the carbon shell combines closely with the nanocores, and significantly enhances the kinetics of lithium intercalation and de-intercalation, as well as the apparent diffusion coefficient of Li-ions. Consequently, the core-shell Si/C nanocomposite exhibits better electrochemical performance than pure Si nanoparticles, indicating that this is a promising approach to improve cyclability and kinetics of nano-anode materials for Li-ion batteries.

Keywords: Li-ion batteries; anode; core-shell; Si/C; emulsion polymerization.

INTRODUCTION

Lithium ion (Li-ion) batteries have long been considered as the most promising back-up power source for a wide variety of modern portable information technology equipment, following their commercial introduction in the early 1990s. So far, many kinds of anode materials have been investigated, such as graphitic carbons [1–3], disordered carbons [4–8], tin-based materials [9–12], nitrides [13], phosphides [14,15], and oxides [16–18]. However, only graphitic carbons are commercially available since the other materials have some disadvantages. For example, in the case of disordered carbons, though their preparation temperature is much lower than that of graphitic carbons and reversible capacity is much larger, there is a serious voltage hysteresis and capacity fading. Nowadays, owing to the rapid advancement of electronic technologies, batteries are required to improve their capacity and cycleability. The latest research is focused on improving and searching for novel synthetic methods of the electrode materials [19–25]. Recently, nanomaterials have attracted much interest as anodes for Li-ion batteries because of their larger reversible capacity, higher Li⁺ diffusion coefficients, and better rate capability than conventional micrometer materials [26–31]. Homogeneous dispersion of nanoparticles in a matrix and synthesis of metal-encapsulated spherical hollow carbon have been explored as approaches to improved cycling behavior [32–34], but it is evident that there is still much scope for further improvement.

*Paper based on a presentation at the 15th International Symposium on Fine Chemistry and Functional Polymers (FCFP-XV) and the 1st International Symposium on Novel Materials and their Synthesis (NMS-I), 17–20 October 2005, Shanghai, China. Other presentations are published in this issue, pp. 1803–1896.

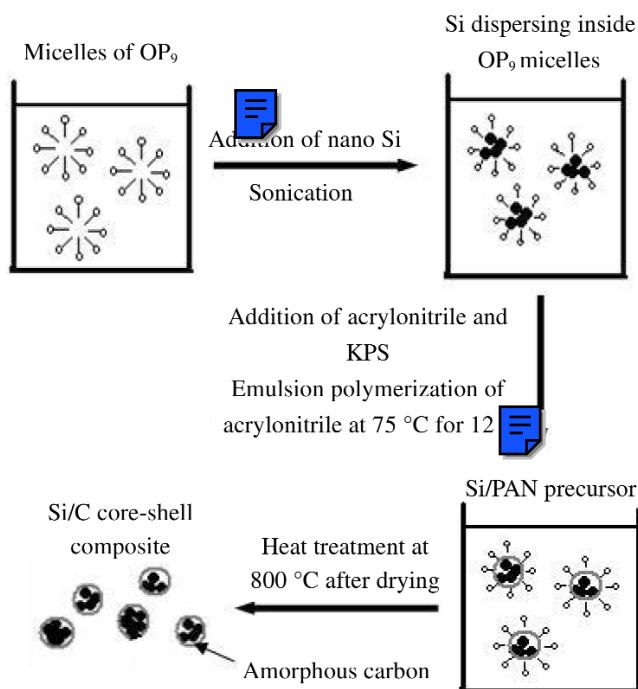
[‡]Corresponding author

Silicon is regarded as one of the most promising candidates as anode material for Li-ion batteries. Its theoretical capacity (4000 mAh g^{-1}) is much higher than that of the commercialized graphite (372 mAh g^{-1}) [19]. However, the cycle performance of silicon is poor, owing to severe volume expansion and shrinkage during Li^+ intercalation and de-intercalation, which results in pulverization of Si particles and eventual loss of Li^+ storage ability [35]. To solve this problem, nanosized Si particles have been utilized and have achieved partial improvement by reducing the absolute volume change. Nevertheless, a new problem was encountered in nanosized material, since fine Si particles aggregate to larger ones during Li^+ insertion/extraction, and the nanocharacteristics then disappear with attendant loss of capacity [36]. Recently, soft matrixes for Si such as carbon [37,38], TiN and TiB_2 [39], and silver [40] were introduced to form composite with Si, however, silicon is still not stable and will separate with the soft matrixes, leading to poor cycling.

In this work, an effective method has been used to synthesize nanosized core-shell carbon-coated Si composite as anode material for Li-ion battery to keep the stability of the electroactive nanoparticles and ameliorate its capacity retention. The kinetics of Li intercalation and de-intercalation has been also investigated.

SYNTHESIS OF CARBON-COATED Si NANOPARTICLES

The synthetic process of carbon-coated Si nanocomposite is shown in Scheme 1. First, a core-shell shaped Si/polyacrylonitrile (PAN) precursor was synthesized via emulsion polymerization. Then, the precursor was heat-treated to turn into core-shell Si/C nanocomposites. One detailed experiment is as follows. OP_9 (1.0 g, as surfactant) was dispersed into deionized water (200 mL) to form micelles. Then, silicon nanoparticles (0.5 g, spherical, $d \leq 50 \text{ nm}$, Zhongchao Company, China) were added and sonicated for 30 min to achieve uniform dispersion. A mixture of acrylonitrile (1.0 g, as monomer) and potassium peroxydisulfate (0.005 g, as initiator) was added for the emulsion polymerization. Degassing



Scheme 1 Synthetic scheme of core-shell Si/C nanocomposite.

was carried out for 1 h under gentle stirring, then the temperature was increased to 75 °C and the mixture was polymerized for 12 h under argon atmosphere to form a core-shell shaped Si/PAN precursor. After centrifugal filtration and drying, the Si/PAN precursor was heat-treated for 6 h at 800 °C to carbonize the PAN to form hard carbon shell, and eventually Si/C nanocomposites were synthesized.

MICROGRAPH AND STRUCTURE OF CARBON-COATED Si NANOPARTICLES

The core-shell Si/C nanocomposite was identified using transmission electronic microscope (TEM) observation and energy dispersive spectrum (EDS) analysis (JEOL JEM 2011). Figure 1a is the TEM micrograph of the carbon-coated Si nanoparticles. It shows that these nanoparticles are linked by carbon shell uniformly, not aggregate together. Figure 1b is the magnification of partial Fig. 1a, showing clearly that the carbon shell was successfully coated on the Si core. Meanwhile, the cores of Si nanoparticles combine closely with the carbon shell, different from the reported carbon coating on tin. In the latter case, the combination of the tin core with the carbon shell is very loose from the transmission electronic micrographs [34]. The thickness of the carbon shell is about 3–5 nm. By changing the ratio of Si and the monomer, and the experimental conditions such as the amount of surfactant and the initiator, the thickness of carbon shell can be adjusted.

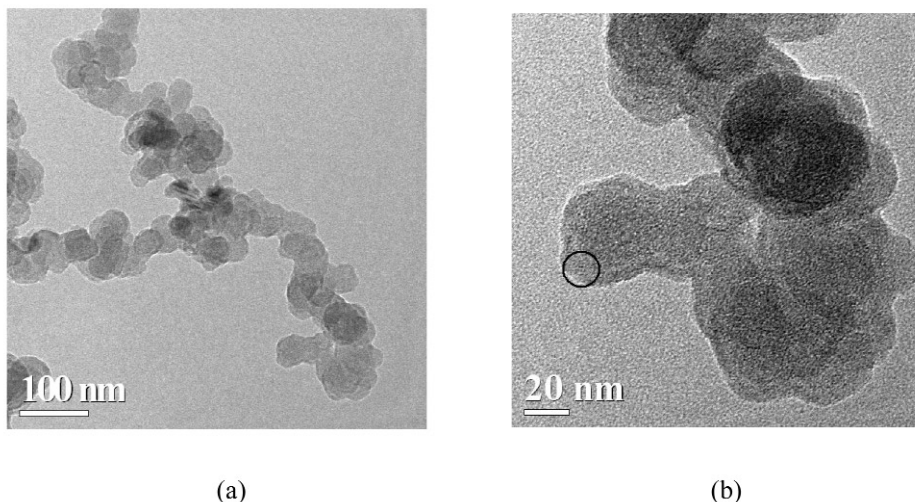


Fig. 1 TEM micrograph of core-shell Si/C nanocomposite (a) and its partial magnification (b).

In order to detect the element composition, EDS pattern was obtained from the shell part of the nanoparticles (the circle area of Fig. 1b). A high carbon peak appeared as shown in Fig. 2, which also confirms the core-shell structure. In addition, our previous studies showed that carbons from heat-treatment of PAN at a temperature <1000 °C are amorphous and consist of a lot of micropores, which can definitely be passages for Li-ions [19,41,42].

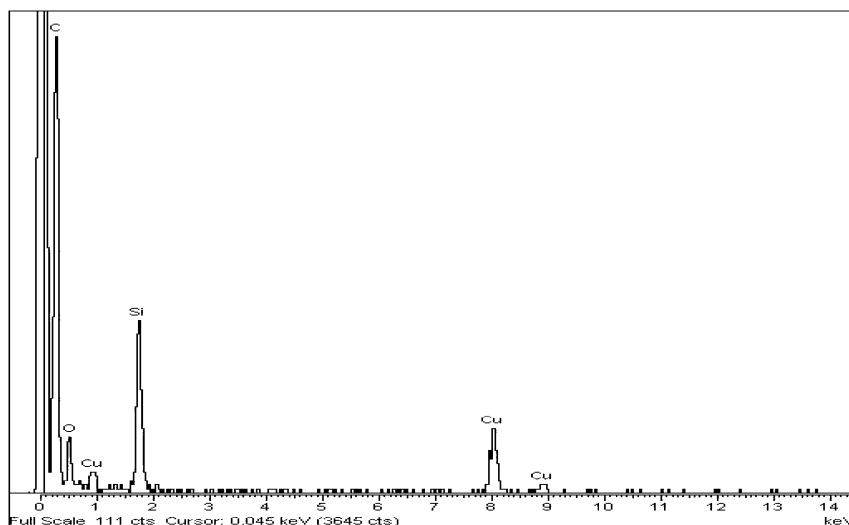


Fig. 2 EDS pattern of the carbon shell of Si/C nanocomposite (the circle area of Fig. 1b).

EVALUATION AS ANODE MATERIALS FOR LI-ION BATTERIES

Two-electrode coin-type half-cells were assembled for electrochemical performance evaluation. Si nanoparticles or Si/C nanocomposites (60 % by mass) were mixed with 20 % acetylene black (AB) as conductive additive and 20 % poly(vinylidene fluoride) as binder. The mixture slurry was coated on copper foil. After drying, it was cut into round pellets with a diameter of about 1 cm and about 10 mg. Using these pellets as working electrode, coin-type model cells were assembled into a glove box filled with argon gas. Li metal was used as the counter electrode, Celgard 2400 as the separator, and 1 mol l⁻¹ LiPF₆ in diethyl carbonate (DEC)/ethylene carbonate (EC)/dimethyl carbonate (DMC) (1:1:1 by mass) solution as the electrolyte. Cycling test of the coin-type half-cells was performed in the voltage range of 0.01–2.5 V with a constant current 0.2 mA cm⁻² at room temperature. Cyclic voltammetry (CV) of Si nanoparticles and Si/C nanocomposite electrodes was measured in the range of 0–2.0 V at scanning rates of 0.1, 0.2, 0.5, and 1.0 mV s⁻¹, respectively.

DISCHARGE AND CHARGE PERFORMANCE

The discharge and charge curves of Si and Si/C electrodes in the first cycle are shown in Fig. 3a. The anode of Si nanoparticles shows a large irreversible capacity about 1200 mAh g⁻¹. In contrast, the irreversible capacity of Si/C nanocomposites is about 600 mAh g⁻¹, only half that of Si. This can be mainly ascribed to the following two aspects. (1) In the case of anode materials, it is necessary to form a solid electrolyte interface (SEI) film by reduction of electrolytes to prevent the reaction of electrolytes with the formed Li insertion (or intercalation) compounds [19]. When the surface area is larger, usually the corresponding area for the SEI film will be larger. When the nanoparticles are coated with carbon shell, the surface area will decrease and the corresponding amount for the SEI film will decrease. (2) The SEI film on carbon surface can be easily formed due to small expansion after Li insertion. In contrast, the expansion of Si during Li insertion results in metastable noncrystalline phases and the accompanying formation of the SEI is almost needed [43].

As mentioned above, the carbon shell is amorphous and Li⁺ can pass through the micropores. It does not affect the electrochemical performance of Si cores. However, it was found that the original reversible capacity of Si/C nanocomposite (1137 mAh g⁻¹) is lower than that of virginal Si nanoparticles

(1831 mAh g⁻¹). The main reason is that the reversible capacity of carbon shell is lower than that of Si [19].

The cycling behavior of Si and Si/C electrodes is shown in Fig. 3b. The anode of Si nanoparticles shows a rapid capacity fading and retains only 6.5 % of the original capacity after 20 cycles. However, in the case of Si/C nanocomposite, after 20 cycles, the charge capacity still remained 52.5 % (594 mAh g⁻¹) of its original capacity (1137 mAh g⁻¹), which is much higher than that of the Si. It shows that the Si/C core-shell nanocomposite has better capacity retention. The main reason is that the coated carbon shell can act as a barrier to prevent the aggregation of Si nanoparticles and thus increase their structure stability during cycling. Of course, the particles of the nanocomposite will also agglomerate during cycling. However, the electroactive Si particles could not combine together due to the existence of the carbon shell. As a result, the nanocharacteristics of the Si particles are reserved during cycling.

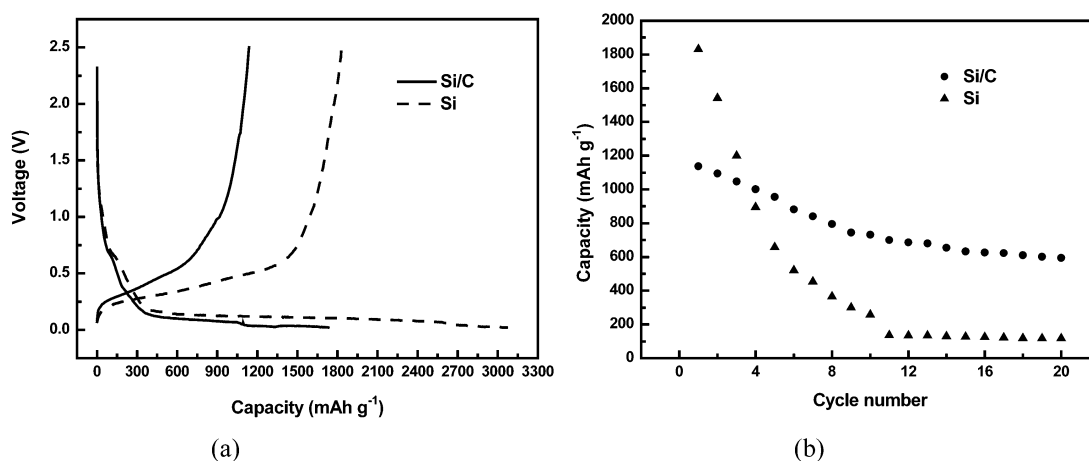


Fig. 3 Electrochemical performance of the core-shell Si/C nanocomposite and the virginal Si nanoparticles cycled between 0.01 and 2.5 V with a constant current of 0.2 mA cm⁻²: (a) the charge/discharge profiles in the first cycle and (b) the cycling behavior.

CYCLIC VOLTAMMETRY

Figure 4 depicts the CVs of Si and Si/C electrodes measured between 0 and 2.0 V at the scanning rate of 0.5 mV s⁻¹. It shows that the oxidation and reduction peak currents (I_p) are much higher than those of the virginal Si nanoparticles, demonstrating a better Li⁺ activity of Si nanoparticles after being coated by a carbon shell. The results from CV data at different scan rates present much more interesting phenomena. We found the oxidation peak current at different scan rate was in proportion to the root of the scan rate, $v^{1/2}$, indicating that the reaction kinetics was controlled by the diffusion step. Moreover, based on the CV data at different scan rate and the following equation:

$$I_p = 2.69 \times 10^5 n^2 A^{2/3} C_0 D^{1/2} v^{1/2} \quad (1)$$

where n is the number of electrons per molecule during the intercalation, A is the surface area of the anode, C_0 is the concentration of Li⁺, D is the diffusion coefficient of Li⁺, v is the scan rate. Since we could not know the real surface of the anode, the geometric surface area of the anode was used, instead. Based on the linear relationship between I_p and $v^{1/2}$ shown in Fig. 5 and eq. 1, the apparent diffusion coefficients of Li ions in both Si/C nanocomposite and Si nanoparticles were calculated. It was found that the diffusion coefficient of Li⁺ in Si/C nanocomposite (9.68×10^{-13} cm² s⁻¹) was about one order

of magnitude higher than that in pure Si nanoparticles ($1.09 \times 10^{-13} \text{ cm}^2 \text{ s}^{-1}$), indicating that the carbon shell at the surface of Si nanoparticles is beneficial for the diffusion of Li^+ since it is conductive. This effect is similar to that of carbon coating on TiO_2 and cathode materials [44–46], which also favors Li intercalation and de-intercalation. Meanwhile, different thickness of the coated carbon shell will present different effects.

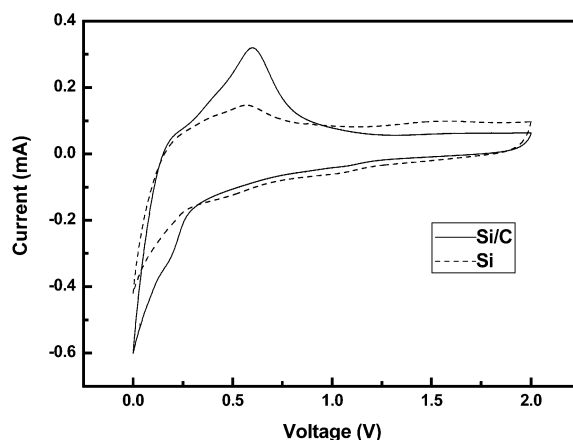


Fig. 4 CV profiles of virginal Si and Si/C electrodes measured at the range of 0–2.0 V with a scanning rate of 0.5 mV s^{-1} .

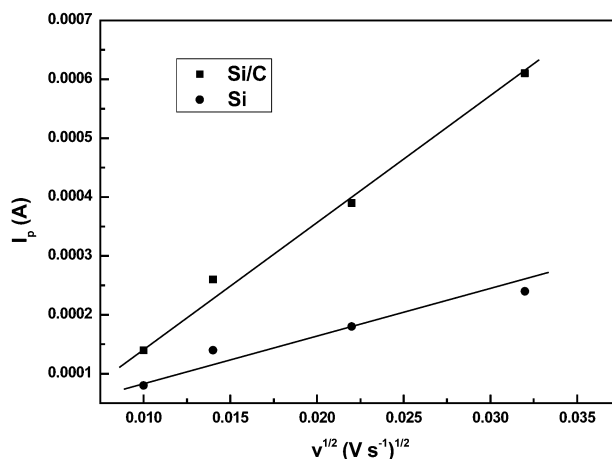


Fig. 5 Relationship between I_p and $v^{1/2}$ of the core-shell Si/C nanocomposite and the virginal Si nanoparticles.

CONCLUSION

Core-shell Si/C nanocomposite was synthesized by emulsion polymerization and following heat-carbonization process. This novel material was used as anode for Li-ion batteries. Data from CV demonstrate clearly that the carbon coating markedly improves the apparent diffusion coefficients of Li^+ , as well as the kinetics of Li intercalation and de-intercalation. The main reason is ascribed to the existence of conductive carbon shells and their close combination with the Si cores. The carbon shell acts as a barrier to suppress the aggregation of Si nanoparticles and thus increases their structure stability during

cycling. Consequently, the capacity retention of the Si nanoparticles is improved obviously. In comparison with former methods [37–40], this method can ensure homogeneous and complete coating of the Si nanoparticles and prevent the Si nanoparticles to contact directly with the electrolytes. It shows that carbon coating is an effective method to improve electrochemical performance of nanoelectrode materials for Li-ion batteries.

ACKNOWLEDGMENTS

Financial support from the China Natural Science Foundation (20474010 and 20333040) and the Shanghai Science & Technology Committee (0452nm064 and 04QMX1406) is greatly appreciated.

REFERENCES

1. M. Mohri, N. Yanagisawa, Y. Tajima, H. Tanaka, T. Mitate, S. Nakajima, M. Yoshida, Y. Yoshimoto, T. Suzuki, H. Wada. *J. Power Sources* **26**, 26 (1989).
2. Y. P. Wu, C. Jiang, C. Wan, R. Holze. *Electrochem. Commun.* **4**, 483 (2002).
3. Y. P. Wu, E. Rahm, R. Holze. *J. Power Sources* **114**, 228 (2003).
4. K. Sato, M. Noguchi, A. Demachi, N. Oki, M. Endo. *Science* **264**, 556 (1994).
5. S. Yata, Y. Hato, H. Kinoshita, N. Ando, A. Anekawa, T. Hashimoto, M. Yamaguchi, K. Tanaka, T. Yamabe. *Synth. Met.* **73**, 273 (1995).
6. Y. P. Wu, S. B. Fang, Y. Y. Jiang. *J. Mater. Chem.* **8**, 2223 (1998).
7. Y. P. Wu, S. B. Fang, Y. Y. Jiang. *Solid State Ionics* **120**, 117 (1999).
8. Y. P. Wu, S. B. Fang, Y. Y. Jiang. *J. Power Sources* **75**, 206 (1998).
9. Y. Idota, T. Kubota, A. Matsufuji, Y. Maekawa, T. Miyasaka. *Science* **276**, 1395 (1997).
10. D. L. Foster, J. Wolfensine, J. R. Read, W. K. Behl. *Electrochem. Solid-State Lett.* **3**, 203 (2000).
11. N. C. Li, C. R. Martin, B. Scrosati. *Electrochem. Solid-State Lett.* **3**, 316 (2000).
12. Y. Wang, J. Y. Lee. *J. Phys. Chem. B* **108**, 17832 (2004).
13. Y. Liu, T. Matsumura, N. Imanishi, T. Ichikawa, A. Hirano, Y. Takeda. *Electrochem. Commun.* **6**, 632 (2004).
14. D. Souza, V. Pralong, A. J. Jacobson, L. F. Nazar. *Science* **296**, 2012 (2002).
15. H. Pfeifer, F. Tancret, M. P. Bichat, L. Monconduit, F. Favier, T. Brousse. *Electrochem. Commun.* **6**, 263 (2004).
16. B. Laik, P. Poizot, J. M. Tarascon. *J. Electrochem. Soc.* **149**, A251 (2002).
17. D. Larcher, G. Sudant, J. B. Leriche, Y. Chabre, J. M. Tarascon. *J. Electrochem. Soc.* **149**, A234 (2002).
18. Y. M. Kang, K. T. Kim, J. H. Kim, H. S. Kim, P. S. Lee, J. Y. Lee, H. K. Liu, S. X. Dou. *J. Power Sources* **133**, 252 (2004).
19. Y. P. Wu, X. B. Dai, J. Q. Ma, Y. J. Chen. *Lithium Ion Batteries: Practice and Applications*, Chemical Industry Press, Beijing (2004).
20. J. Rowsell, V. Pralong, L. Nazar. *J. Am. Chem. Soc.* **123**, 8598 (2001).
21. N. Perira, L. Duppont, J. M. Trarscon, L. C. Klein, G. G. Amatucci. *J. Electrochem. Soc.* **150**, A1272 (2003).
22. H. Jun, M. Park, Y. Yoon, G. Kim, S. Joo. *J. Power Sources* **115**, 346 (2003).
23. T. Matsumura, N. Sonoyama, R. Kanno, M. Takano. *Solid State Ionics* **158**, 253 (2003).
24. L. J. Fu, H. Liu, Y. P. Wu, E. Rahm, R. Holze, H. Q. Wu. *Prog. Mater. Sci.* **50**, 881 (2005).
25. Y. P. Wu, E. Rahm, R. Holze. *Electrochim. Acta* **47**, 3491 (2002).
26. P. Polzot, S. Laruelle, S. Grugeon, L. Dupont, J. M. Tarascon. *Nature* **407**, 496 (2000).
27. H. Kim, J. Choi, H. J. Sohn. *J. Electrochem. Soc.* **146**, 4401 (1999).
28. J. Yang, Y. Takeda, N. Imanishi, O. Yamamoto. *J. Electrochem. Soc.* **146**, 4009 (1999).
29. N. C. Li, C. R. Martin. *J. Electrochem. Soc.* **148**, A164 (2001).

30. D. S. Wu, C. Y. Han, S. Y. Wang, N. L. Wu, I. A. Rusakova. *Mater. Lett.* **53**, 155 (2002).
31. S. Ohara, J. Suzuki, K. Sekine, T. Takamura. *J. Power Sources* **119–121**, 591 (2003).
32. I. Kim, P. N. Kumta, G. E. Blomgren. *Electrochem. Solid-State Lett.* **3**, 493 (2000).
33. S. H. Wang, H. Lee, S. Jang, S. M. Lee, S. J. Lee, H. Baik, J. Lee. *Electrochem. Solid-State Lett.* **4**, A97 (2001).
34. K. T. Lee, Y. S. Jung, S. M. Oh. *J. Am. Chem. Soc.* **125**, 5652 (2003).
35. J. O. Bensenhard, J. Yang, M. Winter. *J. Power Sources* **68**, 87 (1997).
36. H. Li, X. Huang, L. Chen. *Solid State Ionics* **135**, 181 (2000).
37. Y. Zhang, Z. W. Fu, Q. Z. Qin. *Electrochem. Commun.* **6**, 484 (2004).
38. T. Moritaz, N. Takami. *J. Electrochem. Soc.* **153**, A425 (2006).
39. Y. Liu, K. Hanai, T. Matsumura, N. Imanishi, A. Hirano, Y. Takeda. *Electrochem. Solid-State Lett.* **7**, A492 (2004).
40. Y. P. Wu, C. R. Wan, C. Y. Jiang, S. B. Fang. *Lithium Secondary Ion Batteries*, Chemical Industry Press, Beijing (2002).
41. Y. P. Wu, Y. X. Li, S. B. Fang, Y. Y. Jiang. *J. Mater. Sci.* **34**, 4253 (1999).
42. Y. P. Wu, C. R. Wan, S. B. Fang, Y. Y. Jiang. *Carbon* **37**, 1901 (1999).
43. P. Limthongkul, Y. Jang, N. J. Dudney, Y. M. Chiang. *J. Power Sources* **119–121**, 604 (2003).
44. L. J. Fu, H. Liu, H. P. Zhang, C. Li, T. Zhang, Y. P. Wu, R. Holze, H. Q. Wu. *Electrochem. Commun.* **8**, 1 (2006).
45. C. Li, H. P. Zhang, L. J. Fu, H. Liu, Y. P. Wu, E. Rahm, R. Holze, H. Q. Wu. *Electrochim. Acta* **51**, 3872 (2006).
46. L. J. Fu, H. Liu, H. P. Zhang, C. Li, T. Zhang, Y. P. Wu, H. Q. Wu. *J. Power Sources* In press.